Wind Tunnel Study of a “Floating” Wind Turbine’s Wake in an Atmospheric Boundary Layer with Imposed Characteristic Surge Motion

Wind Tunnel Study of a "Floating" Wind Turbine's Wake in an Atmospheric Boundary Layer with Imposed Characteristic Surge Motion

Benyamin Schliffke[1,2], Sandrine Aubrun[2], Boris Conan[2]

1 : Agence de l'Environnement et de la Maîtrise de l'Energie (ADEME), 20 avenue du Grésillé, 49004 Angers Cedex 01, France
2 : LHEEA, Centrale Nantes, 1 rue de la Noë, 44321, Nantes Cedex 3, France

E-mail: benyamin.schliffke@ec-nantes.fr

Abstract. Floating offshore wind turbines (FOWTs) are a potential source for increased offshore energy production. As the technology is still in a pre-industrial state several questions remain to be addressed where little field data is available. This study uses physical modelling at a reduced scale to investigate the unsteady behaviour and the development of the wake in a simplified FOWT model. A porous disc model is placed in an atmospheric wind tunnel and subjected to a range of different motions. The effects of induced sinusoidal surge motion on the characteristics of the model's wake at a fixed downstream distance of 4.6D are studied. First results show unchanged mean velocity values but modified turbulence intensity and turbulent kinetic energy profiles. Spectra taken in the wake show shifts to higher frequencies in the longitudinal flow component while the opposite is true for the vertical flow component. Further research into spatial characteristics of the wake are necessary to confirm these results.

1. Introduction

Floating offshore wind turbines (FOWTs) provide access to higher and steadier winds because they can be placed further offshore, in deeper waters, than their bottom fixed counterparts. Several important questions remain unanswered since the technology is still in a pre-commercial market. A first prototype park has been operational since 2017 in Scotland (Hywind), with several other parks due to come online around Europe in the near future [1]. Apart from several engineering and control questions, the far wake of a floating wind turbine is a field of ongoing research because of its great importance for wind farm design and the performance of individual farms.

Bottom-fixed wind turbines' wakes have been studied extensively in the past decades [2]. Observations made on real or modelled fixed-bottom wind turbines both onshore and offshore show the importance of the properties of the inflow (i.e. turbulence intensity, thermal stability) and the wind turbine orientation with respect to the wind direction (yaw) in the development of the wake. The dynamics of the wake meandering mechanism and its close link to inflow turbulent scales have also been discussed in wind tunnel studies [3–6] and field campaigns [7; 8]).

Regarding FOWTs the literature on engineering aspects or production optimisation is available (see [9] or [10]). Also studies of the near wake have been carried out ([11]). Only recently have studies been published investigating the effects of imposed motion on the characteristics

of the far wake since the motion of the floating platform is expected to interact with the wind turbine wake. In an experimental study using a turbulent boundary layer the effects of pitch and roll motions have been studied [12]. In [13] the effects of wake meandering on the loads experienced by FOWTs are investigated numerically. Surge, pitch and yaw motions are studied for different floaters and different turbulence models. While lateral wake meandering is independent of the floaters used in the study, floater specific characteristics in the vertical wake meandering can be observed. These are linked to a given floater's behaviour in pitch motion, as the wake is directed upwards depending on the pitch angle.

Although individual elements of this work have been investigated before, there is no literature available of experimental work using an actuator disc in modelled atmospheric boundary layer conditions with realistic imposed motion. In this work, sinusoidal surge motion representing realistic frequencies and amplitudes of a floating platform are imposed upon a model installed in an atmospheric wind tunnel reproducing an offshore atmospheric boundary layer at 1/500 scale. The effects of varying frequencies and amplitudes are studied. The questions tackled in this study are: Can the motion's signature be found in the wake? What effect does the imposed surge motion have on the mean and turbulent quantities in the far wake of the turbine model ($> 4\,D$)?

The methodology of the experimental work is described in section 2. The main results obtained so far are presented in section 3. Conclusions and a brief outlook are given in section 4.

2. Methodology

In this work, the model used in the wind tunnel represents a 2 MW floating wind turbine installed on a barge ($80\,m$ rotor diameter, $60\,m$ hub height (h)) similar to FLOATGEN (see [14] for more information), a prototype designed by IDEOL and installed at the SEM-REV test site (Centrale Nantes) that has been operational since September 2018. In the test-section, the wind turbine is modelled by an actuator disc (also called porous disc). The porous disc concept has been validated when studying the wake at distances greater than $x/D > 3$ by verifying that the mean velocity and turbulence intensity as well as higher order statistical moments in the wake of a rotating turbine model and a porous disc are sufficiently similar. If inflow conditions are representative of an atmospheric boundary layer, the rotational momentum and tip vortex signature cannot be detected in the wake at distances greater than $3\,D$ downstream from the model [15]. The actuator disc concept can be applied in low turbulence boundary layers, though at greater distances than $x/D = 3$. The porous disc in this study has a diameter D of $160\,mm$ and a hub height of $120\,mm$. The porous disc is made of the same mesh used in an earlier study [15]. The thrust coefficient C_t is thus estimated to be approximately 0.5 and the power coefficient $C_p \approx 0.25$ (see [15] for more detail on the calculation of C_t and C_p).

2.1. Scaling laws in the wind tunnel

The scaling factors are deduced from wind tunnel constraints and Strouhal similarity. The principal constraints are the size and power of the wind tunnel. It is most important to limit blockage to less than 5 % [16]. In this case another limiting factor comes into play, namely the boundary layer height. It is estimated to be around $3.75\,D$. The actuator disc must be sufficiently small to fit into the boundary layer at least twice to avoid interaction between the free stream and the wake of the turbine. Given a full scale rotor diameter of $80\,m$ and the size of the test section ($24\,m$ length, $2\,m \times 2\,m$ cross-section), the maximum diameter of the porous disc model must therefore be less $30\,cm$. A velocity scaling factor Λ_v is introduced to bring motion frequencies into a manageable range. Taking all constraints into account a geometric scale of $\Lambda_L = 1:500$ and a velocity scale of $\Lambda_v = 1:2.5$ are chosen.

According to Strouhal similarity theory, the following is valid to retain aerodynamic similarity between flows:

$$S_t = \frac{L_{model}}{t_{model} \times U_{model}} = \frac{L_{full\,scale}}{t_{full\,scale} \times U_{full\,scale}} \tag{1}$$

where L, t and U denote a characteristic length, time scale and velocity, respectively, for the model and full-scale cases. From the scaling factors mentioned above the time scaling factor can be derived as follows:

$$\Lambda_t = \frac{\Lambda_L}{\Lambda_v} = 200 \tag{2}$$

A time scaling factor of 200 implies that all processes in the wind tunnel flow happen 200 times faster than at full scale. This has serious implications for the motion system which must be capable of reproducing high frequency motions. At the same time the high frequency motions allow for a faster statistical convergence of average values.

2.2. Motion Modelling

Given the geometric scaling factor of $\Lambda_L = 500$, the velocity scaling factor of $\Lambda_v = 2.5$ and the resulting time scaling factor of $\Lambda_t = 200$, characteristic second order surge motions at model scale were found to be in the order of a few cm at several Hz in the roughest sea states within the operational boundaries of the FOWT. The sea conditions used to derive the floater's motion are related to wind conditions at the wind turbine's upper operational limit ($\approx 30\,ms^{-1}$) at its current location. The wave period is $T_p = 11.37\,s$ with a significant wave height of $H_s = 4.25\,m$. The full-scale equivalent for the characteristic amplitude is $A_{fs} = 10\,m$. Surge is chosen as a point of departure because it presents the largest amplitudes of motion, thus promising the clearest results for a first analysis. Other degrees of freedom (DoF) will be investigated at a later stage.

The motion system is composed of a linear motor capable of moving the model at prescribed characteristic frequencies and amplitudes. The system is placed below the wind tunnel floor inside a sealed box. It is verified that the opening in the floor does not affect the flow inside the test section. No transfer of vibrations from the linear motor to the measurement support system could be detected. The linear motor is controlled by the software provided by the manufacturer (*LinMot Talk 6.5 Build 20170116*). The software allows the user to create time series of positions, accelerations or velocities. Tests with the motion system showed a systematic offset of the real position of the model to the commanded position of $1\,mm$. A near-constant time delay between the assigned motion and the real motion was also observed. As the model's dynamic behaviour is of interest, the offset is not seen as critical, especially as it appears to be independent of the assigned frequency and amplitude.

2.3. The Modelled Boundary Layer

The boundary layer is developed in the wind tunnel using established practices. A trip, spires and perforated metal plates are used to generate large and small scale turbulence in order to recreate, after a development fetch of $\approx 18\,m$, the characteristics of a maritime boundary layer meeting the VDI guidelines reference values for slightly rough terrain [16]. These reference values include turbulence intensity (I) and integral length scale (L_u^x) profiles as well as the roughness length (z_0), the profile exponent (α) and the displacement height (d_0). Velocity measurements are conducted using a *TSI Cobra probe*. This multi-hole probe allows for high frequency measurements ($> 100Hz$) of all three velocity components with a precision of $\pm 0.3\,ms^{-1}$.

Table 1: Adapted from VDI Guideline 3783 [16]. z_0 is the roughness length, α the exponent coefficient, L_u^x the integral length scale and d_0 the zero plane displacement. The centre column contains the VDI reference data for slightly rough terrain. The right hand column shows the values calculated for the modelled boundary layer.

Quantity	Target	Modelled
z_0 $[m]$	10^{-5} to $5 \cdot 10^{-3}$	5.5×10^{-6}
α	0.08 to 0.12	0.1
L_u^x $[m]$	$\approx$ 250	200
d_0 $[m]$	$\approx$ 0	0

The final set-up delivers a slightly rough boundary layer at the upper end of the category as put forth by the VDI (see table 1). As figure 1 shows, the normalised velocity profiles as well as the turbulence intensity profiles follow the expected profile shapes. Further the integral length scale at hub height (L_u^x) is above the crucial factor of two with respect to the wind turbine's diameter (see [17]). At $z = 100\,m$ (full scale) the integral length scale is $L_u^x = 200\,m$, where the VDI Guideline suggests $L_u^x = 250\,m$ for the corresponding $z_0 = 0.01\,m$. These results correspond roughly to the range suggested by VDI Guideline 3783.

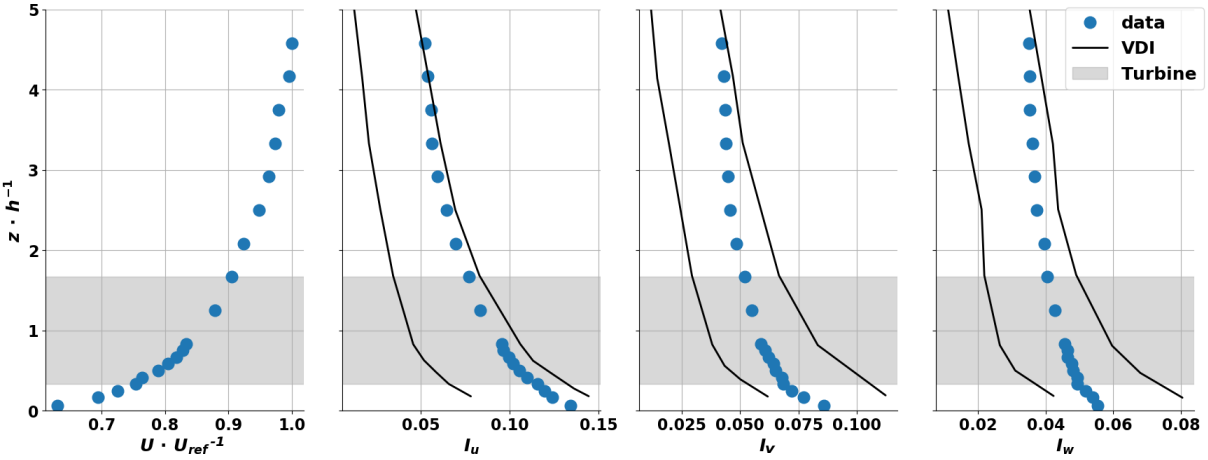

Figure 1: Normalised mean velocity and turbulence intensity profiles of the modelled atmospheric boundary layer. The black lines denote the range of the VDI Guideline's values for slightly rough terrain. The grey area shows the turbine height range. h is the hub height and U_{ref} the reference wind velocity in the wind tunnel.

3. Results

In the following section, the effect of surge motion on the mean wind profile and turbulent kinetic energy (TKE) profile is described at $x = 4.6\,D$ downwind of the wind turbine model. Idealised sinusoidal motion at reduced frequencies (f_{red}) around $f_{red} = 0.10$ with amplitudes varied around $0.125\,D$ are imposed on the model. In order to test the effects of changes in frequency or amplitude on the investigated quantities, a parametric study with frequency and amplitude as variables is carried out. When the effects of frequency changes are investigated the

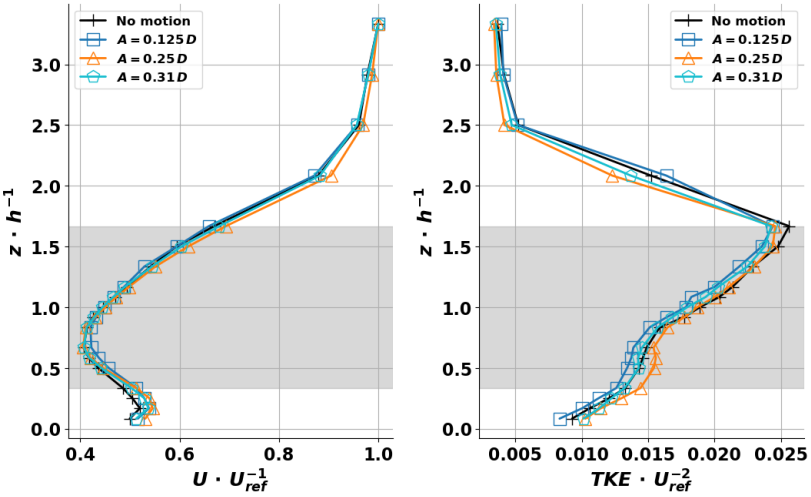

Figure 2: Vertical profiles of the mean normalised velocity (U) and normalised turbulent kinetic energy (TKE). Case: Constant reduced frequency ($f_{red} = 0.10$), varying amplitudes. Measured $4.6\,D$ downstream of the actuator disc.

amplitude is fixed at $A = 0.125\,D$ and the reduced frequency is varied. In the case of amplitude changes $f_{red} = 0.10$ is not changed and the amplitude of the motion is varied. f_{red} is calculated using the following equation:

$$f_{red} = \frac{f \cdot D}{u_{ref}} \tag{3}$$

where f is the input frequency, D is the wind turbine's diameter and u_{ref} is a reference wind velocity, in this study the highest point of each profile. Depending on the test set-up the reference wind velocity is varied between $U_{ref} \approx 3.5\,ms^{-1}$ and $U_{ref} \approx 8\,ms^{-1}$. Turbulence intensity variations are calculated as follows:

$$\Delta I_{x_{gain}} = I_{x_{motion}} - I_{x_{fixed}} \tag{4}$$

where $I_{x_{motion}}$ is the turbulence intensity calculated for a turbine subjected to motion and $I_{x_{fixed}}$ in the fixed turbine case.

3.1. Vertical Profiles

The introduction of idealised sinusoidal surge motion with varying amplitudes or frequency to the wind turbine model does not significantly change the shape of the mean velocity profiles, compared to a fixed turbine's profile (figure 2 and figure 3, right hand panels). $f_{red} = 0.24$ delivers slightly increased mean velocity values beneath $z = h$. With regard to TKE the characteristic motions ($A = 0.125\,D$, $f_{red} = 0.05$, $f_{red} = 0.10$ and $f_{red} = 0.15$) all show decreases compared to the fixed case (black line/crosses) in the area blocked by the turbine (grey area). In the more extreme cases of $A = 0.25\,D$ and $f_{red} = 0.24$ local increases in TKE can be observed (figure 2 and 3, right hand panels).

In order to understand the modified TKE profiles, the turbulence intensity I of each velocity component is studied. The variations of turbulence intensity ($\Delta\, I$) profiles for constant f_{red} are presented in figure 4. The turbulence intensity of the longitudinal component I_u displays an increased spread between the different cases beneath $z = h$, with $A = 0.125\,D$ showing minor

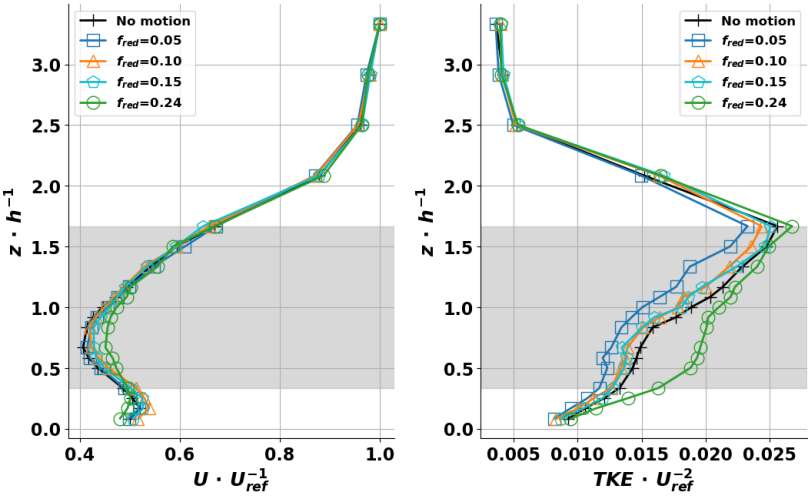

Figure 3: Vertical profiles of the mean normalised velocity (U) and normalised turbulent kinetic energy (TKE). Case: Constant amplitude ($A = 0.125\,D$), varying f_{red}. Measured $4.6\,D$ downstream of the actuator disc.

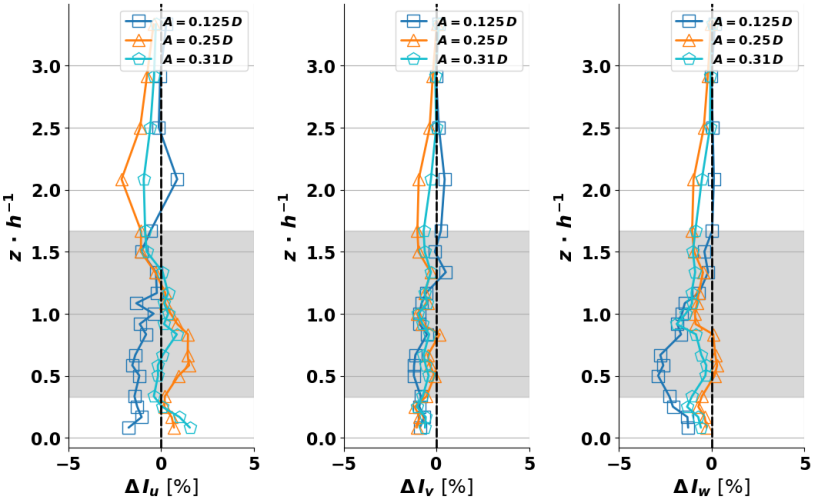

Figure 4: Vertical profiles of the turbulence intensity of each velocity component. Constant reduced frequency (f_{red}), varying amplitudes. Measured $4.6\,D$ downstream of the actuator disc.

losses, $A = 0.31D$ is mostly unchanged, $A = 0.25D$ displaying a slight gain compared to the reference case. This is in line with the observations made in the corresponding TKE profile. This pattern is inverted between $z = 1.5\,h$ and $z = 2.5\,h$. I_v shows a very similar behaviour to the reference case for all measurements. This is to be expected as the surge motion does not have a lateral component. The vertical turbulence intensity (I_w) profile shows losses throughout the profile. The highest losses of I_w are attributed to $A = 0.125\,D$ below $z = h$. Changes in the $A = 0.25\,D$ and $A = 0.31\,D$ profiles are minor compared to the reference case. The tendency to marginal losses in all components may be noted.

Varying f_{red} shows a similar trend to lower turbulence intensities for all velocity components for the characteristic cases ($0.05 > f_{red} > 0.15$). As can be seen in figure 5 the turbulence intensity profiles for all f_{red} for I_u display losses. The largest reductions occur between $z = 0.5\,h$

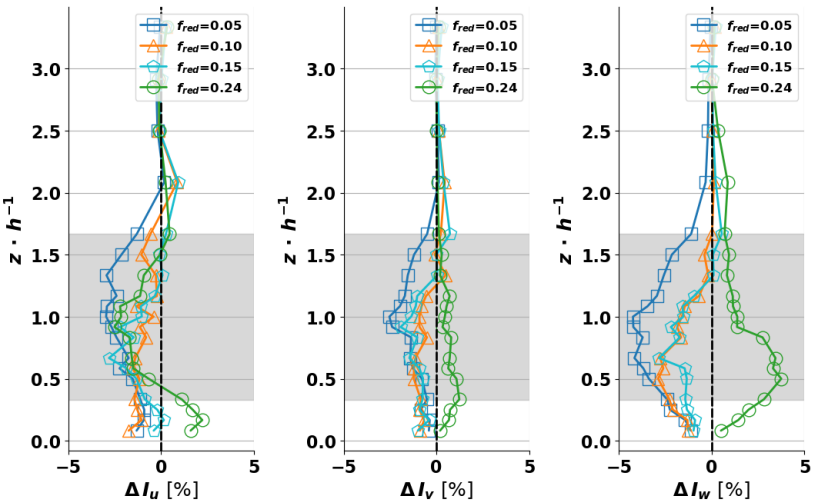

Figure 5: Vertical profiles of the turbulence intensity of each velocity component. Constant amplitude, varying f_{red}. Measured 4.6 D downstream of the actuator disc.

and $z = h$. For I_v reduced frequencies below $f_{red} = 0.15$ lead to reduced turbulence intensities. $f_{red} = 0.24$ shows marginal increases in I_v. Similarly, $f_{red} = 0.24$ shows increased I_w in the bottom half of the profile, where all other f_{red} show a decrease in I_w. Again, $f_{red} = 0.05$ displays the largest reduction in I_w compared to a fixed turbine. It can be concluded that the gains in the TKE profile observed for $f_{red} = 0.24$ in figure 3 can be related to gains in the w component's turbulence intensity seen in figure 5. For the other cases, decreases in TKE and turbulence intensity do not affect the mean velocity in a discernible manner.

3.2. Spectral Content

As the analysis of the profiles show a weak trend, it is necessary to study the spectral content of the wake in order to further substantiate the observations. The spectral content of the flow's longitudinal component (u) at hub height, as shown in figure 6, reveals that the imposed motion frequency can be clearly seen in the far wake. All peaks in the spectrum are associated to the prescribed $f_{red} = 0.10$. When maintaining a constant f_{red} and increasing the amplitude of the motion the peaks become more prominent with increasing amplitudes. The spectra of $A = 0.25\,D$ and $A = 0.31\,D$ have visible first harmonics. A comparison of the spectra indicates that the larger the amplitude, the less broad-band turbulent energy is present in the wake compared to a fixed turbine. This is consistent with the results described in section 3.1.

When maintaining a constant amplitude and varying the reduced frequency, the peaks in the velocity spectra are clearly visible at the expected reduced frequencies (figure 7). $f_{red} = 0.05$ does not have a discernible peak. For all $f_{red} < 0.15$ the spectra are similar to the reference case. The spectrum of $f_{red} = 0.24$ shows decreased large scale turbulence (i.e. lower frequencies), with gains in small scale turbulence (i.e. higher frequencies), when compared to the fixed case. The overall reduction of turbulence in the wake, at the measurement location ($x/D = 4.6$), can be interpreted as an accelerated recovery process, as a return to (lower) inflow turbulence levels is accelerated. The peaks in the spectra grow with increased f_{red}. The crests of the spectra are all located near the crest of the atmospheric boundary layer spectrum at $f_{red} \approx 0.2$. Enhanced interaction between the wake and the surrounding flow can be expected, as both spectra have crests around $St = 0.2$. This may allow for interference between the wake and boundary layer flows.

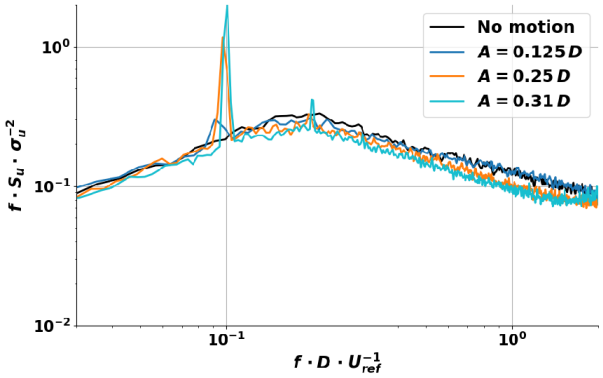

Figure 6: Spectra of the longitudinal velocity component at hub height. Constant reduced frequency (f_{red}), varying amplitudes. Measured 4.6 D downstream of the actuator disc.

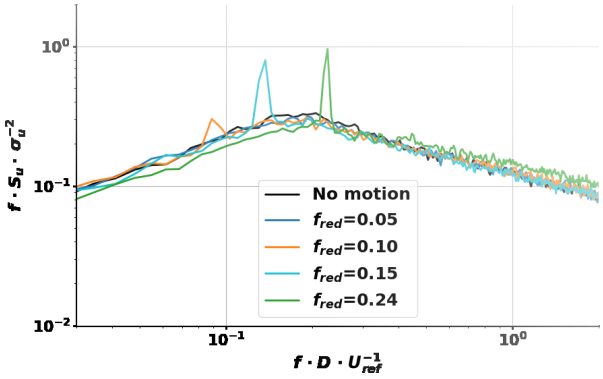

Figure 7: Spectra of the longitudinal velocity component at hub height. Constant amplitude, varying f_{red}. Measured 4.6 D downstream of the actuator disc.

4. Conclusions and Outlook

In the scope of this study the wake of a model wind turbine with imposed surge motion in an atmospheric boundary layer is studied. The measurements are carried out at $x = 4.6\,D$ downstream of the model on the centre line. An actuator disc is used to represent the wind turbine.

First experimental results suggest a mildly enhanced wake under certain, rather extreme, motion regimes. Indications can be found in the reduced turbulence intensity in all but one case ($f_{red} = 0.24$). The same can also be said of the reduced TKE found in the wake in most cases, again $f_{red} = 0.24$ being the exception. The spectral content further underlines this tendency because the energy content in the spectrum is reduced for changing amplitudes or see a shift from low frequency to high frequency turbulence in the case of motion at $f_{red} = 0.24$. These observations are in line with results from other campaigns testing other DoFs (e.g. [12]). Reduced turbulence intensities and reduced TKE would result in lower fatigue loads on an FOWT in a hypothetical second row of turbines. These observations require verification by further measurements. To this avail PIV measurements with good spatial resolution will be conducted allowing a better understanding of wake recovery processes. This, in turn, will lead to a better understanding of the temporal and spatial characteristics of the wake of an FOWT. TKE budget and production analyses are planned to quantify possible enhanced entrainment. The results from PIV measurements can also be compared to results from [13] regarding wake

characteristics.

Acknowledgements
This work was carried out within the framework of the WEAMEC, West Atlantic Marine Energy Community, and with funding from the Pays de la Loire Region, France.

References

[1] Floating Offshore Wind Energy - A Policy Blueprint for Europe https : / / windeurope . org / wp-content / uploads / files / policy / position-papers / Floating-offshore-wind-energy-a-policy-blueprint-for-Europe.pdf accessed: 2020-05-27

[2] Porté-Agel F, Bastankhah M and Shamsoddin S 2019 *Boundary-Layer Meteorology* 1–59

[3] Vermeer L, Sørensen J N and Crespo A 2003 *Progress in aerospace sciences* **39** 467–510

[4] Espana G, Aubrun S, Loyer S and Devinant P 2011 *Wind Energy* **14** 923–937

[5] Espana G, Aubrun S, Loyer S and Devinant P 2012 *Journal of Wind Engineering and Industrial Aerodynamics* **101** 24–33

[6] Chamorro L P and Porté-Agel F 2009 *Boundary-layer meteorology* **132** 129–149

[7] Machefaux E, Larsen G C, Troldborg N, Gaunaa M and Rettenmeier A 2015 *Wind Energy* **18** 2085–2103

[8] Garcia E T, Aubrun S, Coupiac O, Girard N and Boquet M 2019 *Renewable energy* **130** 1–11

[9] Sebastian T and Lackner M 2013 *Wind Energy* **16** 339–352

[10] Rodrigues S, Pinto R T, Soleimanzadeh M, Bosman P A and Bauer P 2015 *Energy conversion and management* **89** 933–941

[11] Bayati I, Belloli M, Bernini L and Zasso A 2017 *Energy Procedia* **137** 214–222

[12] Fu S, Jin Y, Zheng Y and Chamorro L P 2019 *Applied Energy* **253** 113605

[13] Wise A S and Bachynski E E 2020 *Wind Energy* **23** 1266–1285

[14] FLOATGEN Press Kit https://floatgen.eu/sites/default/files/medias/press_kit_-_floatgen.pdf accessed: 2020-05-27

[15] Aubrun S, Loyer S, Hancock P and Hayden P 2013 *Journal of Wind Engineering and Industrial Aerodynamics* **120** 1–8

[16] VDI 2000 Umweltmeteorologie - Physikalische Modellierung von Strömungs- und Ausbreitungsvorgängen in der atmosphärischen Grenzschicht - Windkanalanwendungen Tech. rep. VDI Verein Deutscher Ingenieure e.V. VDI-Platz 1, 40468 Düsseldorf, Germany

[17] Larsen G C, Madsen H A, Thomsen K and Larsen T J 2008 *Wind Energy: An International Journal for Progress and Applications in Wind Power Conversion Technology* **11** 377–395